SOLID POLYMER ELECTROLYTES FROM CROSSLINKED PEG AND DILITHIUM *N,N′*-BIS(TRIFLUOROMETHANESULFONYL)-PERFLUOROALKANE-1,ω-DISULFONAMIDE AND LITHIUM BIS(TRIFLUOROMETHANESULFONYL)IMIDE SALTS

Olt E. GEICULESCU[a1,*], Rama V. RAJAGOPAL[a2], Emilia C. MLADIN[b1], Stephen E. CREAGER[a3] and Darryl D. DESMARTEAU[a4]

[a] *Department of Chemistry, Clemson University, Clemson, SC 29634, U.S.A.; e-mail: [1] oltg@clemson.edu, [2] rrama@clemson.edu, [3] screage@clemson.edu, [4] fluorin@clemson.edu*

[b] *Mechanical Engineering Department, Polytechnical University, 060042 Bucharest, Romania; e-mail: cerna@eeee.unesco.pub.ro*

Received May 13, 2008
Accepted October 10, 2008
Published online December 15, 2008

Dedicated to Professor Oldřich Paleta on the occasion of his 70th birthday in recognition of his outstanding contributions to the area of organofluorine chemistry.

The present work consists of a series of studies with regard to the structure and charge transport in solid polymer electrolytes (SPE) prepared using various new bis(trifluoromethanesulfonyl)imide (TFSI)-based dianionic dilithium salts in crosslinked low-molecular-weight poly(ethylene glycol). Some of the thermal properties (glass transition temperature, differential molar heat capacity) and ionic conductivities were determined for both diluted (EO/Li = 30:1) and concentrated (EO/Li = 10:1) SPEs. Trends in ionic conductivity of the new SPEs with respect to anion structure revealed that while for the dilute electrolytes ionic conductivity is generally rising with increased length of the perfluoroalkylene linking group in the dianions, for the concentrated electrolytes the trend is reversed with respect to dianion length. This behavior could be the result of a combination of two factors: on one hand a decrease in dianion basicity that results in diminished ion pairing and an enhancement in the number of charge carriers with increasing fluorine anion content, thereby increasing ionic conductivity while on the other hand the increasing anion size and concentration produce an increase in the friction/entanglements of the polymeric segments which lowers even more the reduced segmental motion of the crosslinked polymer and decrease the dianion contribution to the overall ionic conductivity. DFT modeling of the same TFSI-based dianionic dilithium salts reveals that the reason for the trend observed is due to the variation in ion dissociation enthalpy, derived from minimum-energy structures, with respect to perfluoroalkylene chain length.

Keywords: LiTFSI; Dilithium *N,N′*-bis(trifluoromethanesulfonyl)perfluoroalkane-1,ω-disulfonamide salts; Cross-linked poly(ethylene glycol); Solid polymer electrolyte; Ionic conductivity; PEG.

doi:10.1135/cccc20081777

Ionic conductivity in solvent-free solid polymer electrolytes based on alkali metal salt complexes with polyethers has been broadly studied both by academia and industrial R&Ds [1–5] because of the applications envisioned for such materials in electrochemical power sources and devices[6–9]. The SPEs have many advantageous properties for such applications, including good dimensional and thermal stability, a wide electrochemical stability window, better shape flexibility and manufacturing integrity and improved safety[10]. Among the polyethers, poly(ethylene oxide) (PEO) complexes of alkali metal salts (especially of lithium) have been extensively studied, due to the fact that the polar main chain ether groups easily coordinate with salt cations in a manner similar to crown ethers, forming a homogeneous solution. This implies that the spacing and conformational flexibility provided by the PEO unit, (CH_2CH_2O), are optimal for coordination with the cation, the PEO unit acting like a Lewis base and the cation as a Lewis acid[10]. To summarize, the host polymer has on one hand to provide a source of electrons capable of facilitating ion separation by solvating the cations of the salt and, on the other hand, to serve as a dynamically mobile background matrix[11].

Unfortunately, the conductivities of high-molecular-weight PEO-based electrolytes at low temperatures is reduced by crystallization of the polymer, especially for the low-salt-content SPEs [12]. Studies led in 1980s established that ionic conduction was confined to the amorphous phase of the polymer electrolytes above their glass transition temperature[13–15]. Several routes have been investigated to prevent crystallization such as block copolymerization[16,17], grafting[18,19] or crosslinking[20,21], which allows one to incorporate PEO into a macromolecular sequence that it will resist host crystallization. We should mention here, for completeness, that just recently it has been claimed that some low-molecular-weight PEO-based crystalline polymer electrolytes not only conduct, but do so better than analogous amorphous phases[22–24].

Poly(ethylene glycol) (PEG) crosslinking was reported to give the polymer a rubber-like texture, large amorphous phase which enhances its ionic conductivity and prevents the material from creeping[20,21]. Cheradame et al.[25] have concentrated on forming chemically crosslinked SPEs which both inhibited crystallization and exhibited good mechanical properties to be fabricated as strong films or membranes. Also, several other groups studied network SPEs based on PEO linked by isocyanates[26–28]. Consistently, conductivities of the network systems were some two orders of magnitude lower than those recorded for salts just dissolved in the polymeric host. This observation reflects the fact that a crosslinked matrix can impede ion transport more than a non-crosslinked one.

Also, the research has concentrated in synthesizing new lithium salts containing a large anion with a highly delocalized negative charge which exhibit a lower lattice energy that make them easier to be solvated by the host polymer[6,29]. Salts consisting of a large anion with delocalized negative charge are particularly desired, and among such salts, those based on the bis(trifluoromethanesulfonyl)imide anion (e.g., TFSI), have been particularly emphasized[27,29–38]. The TFSI anion has a delocalized negative charge and very low basicity which leads to good salt dissociation, less ion pairing, and high ionic conductivity in PEO-based electrolytes[29,32,39]. It is also thought that the TFSI anion exhibits a plasticizing effect on the PEO host, which could contribute to higher SPE conductivity[40]. Most prior work on lithium salt SPEs has concentrated on monoanionic salts[29,41–44].

The present study considers SPEs prepared from crosslinked low-molecular-weight PEG and four new dilithium salts based on dianions with structures similar to that of the TFSI anion[45,46]. The dianion in each of the new salts consists of two discrete anionic units based on a TFSI motif that are linked to each other by a perfluoroalkylene chain. The specific structures of the four dilithium salts are illustrated in Scheme 1.

LiTFSI	$CF_3SO_2N(Li)SO_2CF_3$	**R** - CF_3
Dilithium Salt	$CF_3SO_2N(Li)SO_2(CF_2)_xSO_2N(Li)SO_2CF_3$	**R** - $(CF_2)_x$ – **R**

SCHEME 1
The new lithium salts used in SPEs preparation (R = $CF_3SO_2N(Li)SO_2$-) with a different-length linker: x = 2 (salt **1**), 4 (salt **2**), 6 (salt **3**), 8 (salt **4**)

The work focuses both on thermal/electric characterization of the resulting SPEs as a function of temperature and on the electronic structure and ion dissociation energy calculation for all the dilithium salts by using the density functional theory (DFT). All of the SPEs studied were found to obey the Vogel–Tammann–Fulcher (VTF) correlation describing the temperature dependence of ionic conductivity in glassy ionic conductors. Conductivities for SPEs prepared from the dilithium salts were consistently lower than that of SPEs prepared from monomeric LiTFSI at all temperatures, which probably reflects a diminished contribution of the dianions to the overall conductivity in the dilithium salt SPEs.

EXPERIMENTAL

Materials

The low-molecular-weight polymer hosts such as poly(ethylene glycol) (PEG with average molecular weight of 2,000, melting temperature of 58 °C), and poly(ethylene glycol) methyl ether (PEGME with average molecular weight of 2,000, melting temperature of 52 °C) were provided by Aldrich, while the poly(ethylene glycol) dimethyl ether (PEGDME with average molecular weight of 500) was provided by AlfaAesar. The crosslinker, a 27 wt.% solution of 4,4′,4″-methylidynetris(phenyl isocyanate) (molecular weight of 367, commercial name Desmodur RE) in ethyl acetate was supplied by Bayer AG. The reference salt, lithium bis-(trifluoromethanesulfonyl)imide (LiTFSI) was obtained from 3M Corporation, while all the new dilithium salts, illustrated in Scheme 1, were synthesized according to Scheme 2 [10,47,48], and purified at Clemson by DesMarteau's group using methods that have been described in detail elsewhere[48,49]. Prior to use, LiTFSI was dried first for 24 h at 150 °C and then for 1 h at 170 °C, while all of the dilithium salts were dried for 24 h at 100 °C under dynamic vacuum (2×10^{-2} torr). The polymer hosts were used as received.

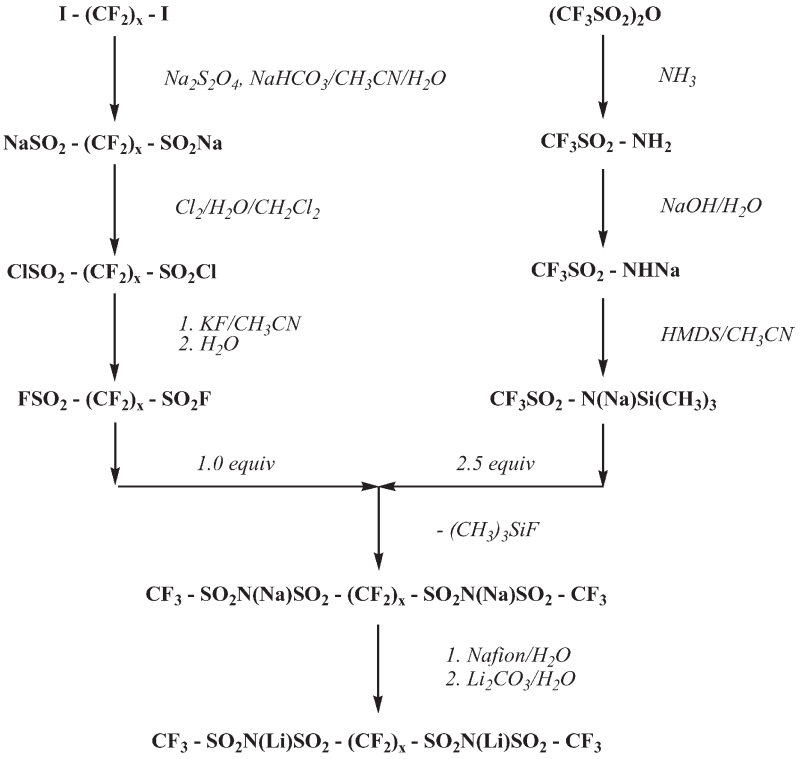

SCHEME 2
General synthetic route for the new dilithium salts used in SPEs preparation (x = 2, 4, 6, 8)[48]

Solid Polymer Electrolytes Preparation

Crosslinked PEG-based electrolytes were prepared using LiTFSI and the dilithium salts **1**–**4** in concentrations corresponding to EO/Li ratios of 10:1 and 30:1. The crosslinking chemistry is described in Scheme 3. First, the necessary amounts of PEG and Li salt were mixed together in the dry box for 1 h at 70 °C on a hot plate. A stoichiometric quantity of crosslinker/PEG of 2:3 mol/mol was added and the mixture was stirred for 30 min at the same temperature. Next, for the crosslinking to take place, the mixture was pressed between two Teflon sheets, and the entire assembly was introduced into a vacuum oven for 2 h at 90 °C under a small flow of nitrogen. The resulting electrolyte membranes could be easily peeled off the Teflon sheets.

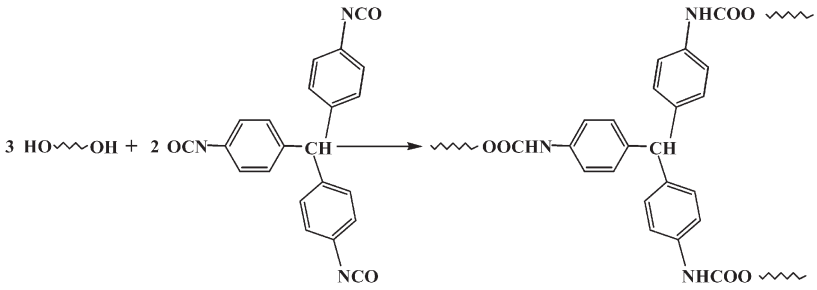

SCHEME 3
General crosslinking chemistry between low-molecular-weight PEG and 4,4′,4″-methylidynetris(phenyl isocyanate) with formation of a polyurethane network[48]

Electrochemical Impedance Spectroscopy (EIS)

SPEs ionic conductivities were measured as a function of temperature by electrochemical impedance spectroscopy (EIS) using a two-electrode cell configuration. As a general procedure, each sample was first heated to 120 °C and then slowly cooled to room temperature, and impedance spectra were recorded on the cooling curve in discrete steps every approximately 10 °C until room temperature was reached.

The SPE resistance at each temperature was obtained from the complex-plane impedance plot by fitting the low-frequency portion of the data to a linear function and taking the intercept of the plot on the real axis as being indicative of the membrane resistance[42,50,51]. Ionic conductivity values κ (in S/cm) were obtained by correcting the membrane impedance for geometric effects using the apparent electrode area and the SPE thickness[48,52,53].

Differential Scanning Calorimetry (DSC)

Thermal properties were studied for each SPE sample after being subjected to EIS measurements, using modulated differential scanning calorimetry (MDSC) performed on a TA Instruments DSC 2920 calorimeter connected, for data analysis, to a TA Instruments Thermal Analyst 3100 workstation. The general procedure involved first heating the samples from room temperature to 120 °C at a rate of 10 °C/min, followed by rapid cooling to –80 °C at a rate of –20 °C/min. Samples were equilibrated at –80 °C for 5 min and then the temperature

was increased to 120 °C at a rate of 5 °C/min. During the last step the temperature was modulated ±1.0 °C every 60 s. The glass transition temperature, T_g (in °C), was taken to be the mid-point temperature of the baseline shift measured during the transition. Also, the heat capacity was measured for all the SPEs using a standard sapphire sample for calibration[48]. Values of C_p (in J/mol K) were determined at 10 K intervals and compared with the values obtained for a standard sapphire sample. Both were measured relative to the baseline established for an empty pan of the same weight as that used for both polymer and the sapphire standard. From these thermograms the change in molar heat capacity at the glass transition temperature, ΔC_p (in J/mol K), was also measured and used to calculate the apparent activation energy of the segmental motion of the polymer.

RESULTS AND DISSCUSION

The ionic conductivity of polymeric electrolyte systems comprising a network of PEG, PEG and PEGME (1:1 mol/mol), or PEG and PEGDME (1:1 mol/mol) crosslinked with 4,4′,4″-methylidynetris(phenyl isocyanate) and containing LiTFSI was studied (EO/Li = 30:1). The results, presented in Fig. 1, show that ionic conductivity increases with the decrease in crosslinking density from SPEs based on PEG (100% crosslinking), to PEG-PEGME (75% crosslinking), and to PEG-PEGDME (50% crosslinking), which was due to an increase in the chain segmental mobility, which is consistent with similar observations by other researchers[54]. Also, it has to be mentioned that with the decrease in the degree of crosslinking, the SPEs increasingly lost their mechanical and dimensional stability.

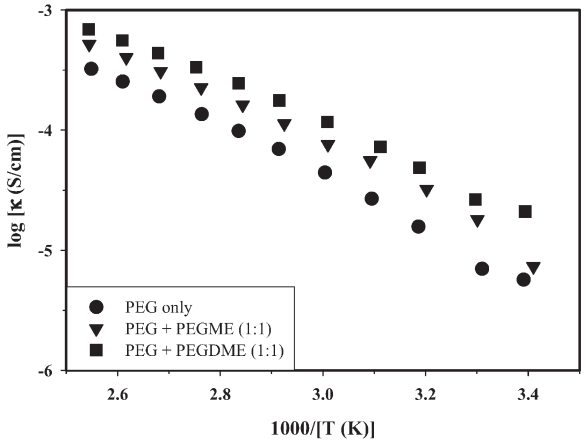

FIG. 1
Arrhenius plots for SPEs made of LiTFSI and crosslinked PEG, PEG–PEGME (1:1 mol/mol) or PEG–PEGDME (1:1 mol/mol), EO/Li = 30:1

LiTFSI and lithium salts **1**–**4** were used to prepare SPE membranes by dissolving the salt in the low-molecular-weight PEG (M = 2,000) and then cross-linking it with 4,4′,4″- methylidynetris(phenyl isocyanate) as shown in Scheme 3 (membrane thicknesses achieved were 300–1,000 μm). The same EO/Li ratios as for the previously studied PEO-based SPEs were used

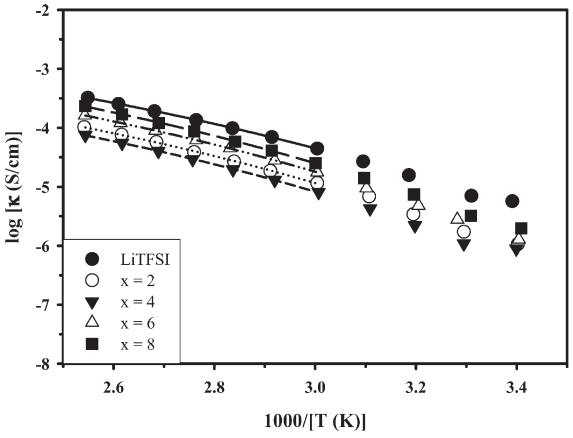

FIG. 2
Arrhenius plots for SPEs made of LiTFSI or a dimeric lithium salt and crosslinked PEG, EO/Li = 30:1

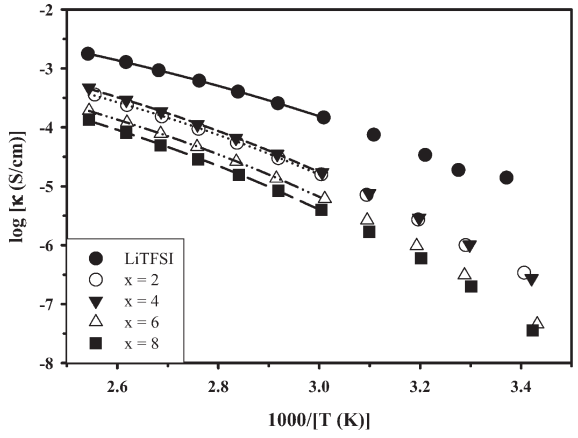

FIG. 3
Arrhenius plots for SPEs made of LiTFSI or a dimeric lithium salt and crosslinked PEG, EO/Li = 10:1

for the preparation of both diluted (30:1) and concentrated (10:1) electrolytes. Following the procedures already described[48,52,53], for all the newly prepared SPEs were obtained the Arrhenius curves (Figs 2 and 3) by EIS and thermograms by MDSC (Figs 4 and 5).

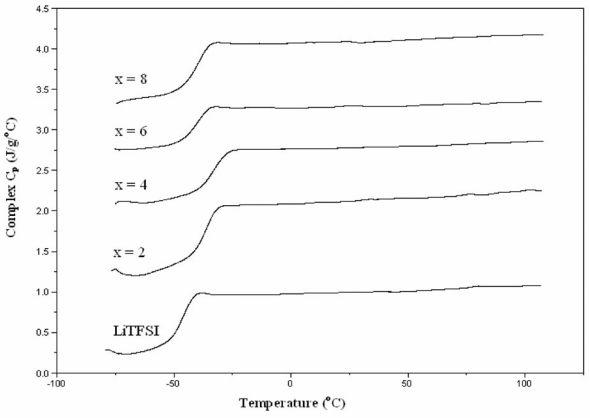

FIG. 4
DSC thermograms for SPEs made of LiTFSI or a dimeric lithium salt and crosslinked PEG, EO/Li = 30:1

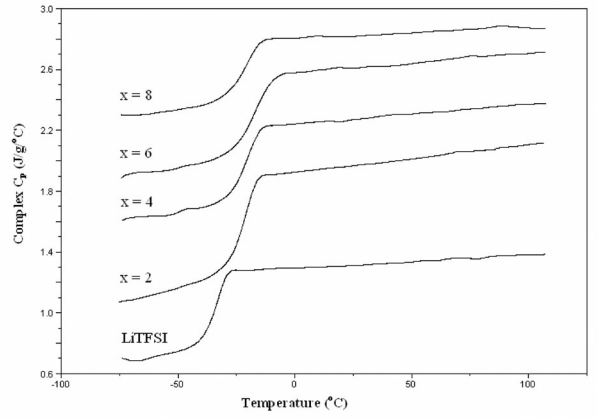

FIG. 5
DSC thermograms for SPEs made of LiTFSI or a dimeric lithium salt and crosslinked PEG, EO/Li = 10:1

Thermal properties such as glass transition temperature (T_g) and differential molar heat capacity (ΔC_p) were determined from the MDSC thermograms. The differential molar heat capacity values were corrected for the salt content and the corresponding corrected values of the differential molar heat capacity, $\Delta C_p^{corr} \pm \sigma$, were calculated to be 32.4 ± 1.6 J/mol K for diluted SPEs (EO/Li = 30:1) and 40.0 ± 1.2 J/mol K for concentrated SPEs (EO/Li = 10:1).

LiTFSI-based electrolytes exhibited the highest ionic conductivity for the entire temperature and concentration ranges. For LiTFSI and salts **1**–**3**, less salt **4** (x = 8), the ionic conductivities are higher for the concentrated SPEs (EO/Li = 10:1, Fig. 3) relative to the dilute SPEs (EO/Li = 30:1, Fig. 2) over the entire temperature range of interest (60–120 °C). This was also partially observed for the PEO-based SPEs when using the same lithium salts[47], but to a lesser extent, and reflects the fact that there are significantly more charge carriers present in the more salt-rich SPE membranes. Also, when compared to the PEO-based SPEs, the crosslinked PEG-based electrolytes exhibited conductivities lower by up to one and a half order of magnitude over the entire temperature range and for both concentrations[47].

It can be observed from Fig. 2 for diluted SPEs, that the electrolyte based on monomeric LiTFSI still has the highest conductivity followed in order by those prepared using the dilithium salts with x = 8, 6, 2 and 4, in the same order as seen for the PEO-based SPEs using the same salts and the same EO/Li ratio[10,48]. Also, no transition in ionic conductivity can be observed around 58 °C, the melting temperature of PEG, which indicates that all these SPEs are probably completely amorphous, which is confirmed by the corresponding DSC thermograms in Fig. 4. This is a major difference compared with the behavior of PEO-based SPEs using the same salts[10,47,48,52] where such a transition was observed at around 60 °C and was attributed to a crystalline melting/freezing transformation of the PEO host.

Therefore, for dilute SPEs, the increasing ionic conductivity with the higher fluorine content in the salt molecule indicates that an increase in anion size, while decreasing the anion contribution to the overall conductivity[38], is increasing the same conductivity by decreasing the anion basicity through electron delocalization which led to a good salt dissociation and less ion-pairing.

Figure 3 shows the Arrhenius plots for the same dilithium salts-based SPEs but with an EO/Li ratio of 10:1. While the electrolyte containing LiTFSI still has the highest ionic conductivity the general trend for SPEs containing the dimers **1**–**4** is the opposite of that one encountered for the diluted PEG- and PEO-based SPEs[47]. Ionic conductivity is decreasing with

the *x* value for the entire temperature range which could signify that with the increase in size and concentration additional entanglements/frictions could appear between the bigger anion and the crosslinked matrix. Also, as can be seen from the thermograms in Fig. 5 all these SPEs are completely amorphous.

Furthermore, all of the Arrhenius curves reveal a slight curvature over the temperature region of interest (60–120 °C), commonly observed in SPEs and in most glassy ionic conductors, which is indicative of the coupling between ion transport and polymer host mobility[55]. The curved Arrhenius plots were fitted using the semi-empirical VTF correlation as described previously[10,47,48]:

$$\kappa = AT^{-1/2} \exp\left[-\frac{B}{(T - T_0)}\right] \qquad (1)$$

in which the phenomenological parameters *A* and *B* are related to the charge carrier concentration and to the apparent activation energy opposing the rearrangement of the polymer segmental unit, respectively. The *B* parameter was further employed to compute the apparent activation energy ($\Delta\mu \pm \sigma$) using the configurational entropy model[56,57]:

$$B = \frac{\Delta\mu S_c^* T_0}{k_B \Delta C_p^{\,\mathrm{corr}} T_g} \qquad (2)$$

where k_B is the Boltzmann constant, S_c^* the minimum configurational entropy required for a cooperative rearrangement of a polymer chain segment involved in ion transport in the matrix (generally taken as k_B ln 2). The term T_0 is referred as either "ideal" or "equilibrium" glass transition temperature, i.e. the temperature at which the configurational entropy approaches zero.

The curved lines in Figs 2 and 3 correspond to nonlinear least-squares fits of the data to the VTF equation using for the equilibrium glass transition temperature (T_0) a value 25 K lower than the glass transition temperature (T_g) value determined by DSC [58]. The best-fit values of *A*, *B* and $\Delta\mu \pm \sigma$ are given in Tables I (EO/Li = 30:1) and II (EO/Li = 10:1) along with the corresponding T_g values.

Looking into the *A*, *B* and $\Delta\mu$ values from the VTF fits in Tables I and II shows us some of the possible rationale for their behavior. Though still the

primary difference among the various salts lies in the *A*-values, they are less diminished with respect to LiTFSI when compared to PEO-based SPEs using the same salts[10,47,48]. This suggests that yet the major cause of the diminished conductivity remains the fact that there are fewer mobile charge carriers present in the dilithium salt SPEs, but their concentration is lower due to the crosslinking, especially for LiTFSI. With regard to the *B*-term from the VTF fits and the apparent activation energy, Δμ, generally they are not anymore diminished relative to that for LiTFSI which may indicate that all these salts did not affect the local microstructure of the host polymer. Due to the PEG crosslinking, which makes the matrix more rigid, both LiTFSI and the dilithium salts **1**–**4** are not having anymore such a strong plastic-

TABLE I
DSC/VTF parameters and the apparent activation energy (Δμ) for SPEs made of LiTFSI or a dimeric lithium salt and crosslinked PEG (EO/Li = 30:1)

Salt type *x*	T_g °C	*A* $K^{1/2}$ S/cm	*B* K	Δμ ± σ kJ/mol	Li salt concentration wt.%
LiTFSI	–45	0.57	853	45.6 ± 2.3	17.9
2	–36	0.19	827	42.9 ± 2.2	16.9
4	–33	0.13	802	41.9 ± 2.1	19.4
6	–40	0.36	876	46.4 ± 2.3	21.8
8	–40	0.56	894	46.6 ± 2.3	24.1

TABLE II
DSC/VTF parameters and the apparent activation energy (Δμ) for SPEs made of LiTFSI or a dimeric lithium salt and crosslinked PEG (EO/Li = 10:1)

Salt type *x*	T_g °C	*A* $K^{1/2}$ S/cm	*B* K	Δμ ± σ kJ/mol	Li salt concentration wt.%
LiTFSI	–33	4.9	880	56.0 ± 1.7	39.5
2	–22	2.2	953	61.9 ± 1.8	37.9
4	–20	3.1	969	62.6 ± 1.9	42.0
6	–17	1.3	949	61.0 ± 1.8	45.7
8	–20	1.3	1036	65.6 ± 1.9	48.7

izing effect upon the polymeric matrix as in the case of PEO. This is easy to observe by looking at the corrected differential molar heat capacity values (ΔC_p^{corr}) which measure the change in polymer molar heat capacity at the glass transition temperature. For PEO-based SPEs ΔC_p^{corr} increased from 11.6 ± 0.7 J/mol K (EO/Li = 30:1) to 52.0 ± 1.8 J/mol K (EO/Li = 10:1), an almost five-fold increase[10,48], while for crosslinked PEG-based SPEs it just barely increased from 32.4 ± 1.6 J/mol K (EO/Li = 30:1) to 40.0 ± 1.2 J/mol K (for EO/Li = 10:1). Analyzing the data in Figs 2 and 3 and Tables I and II reveals some familiar trends with respect to anion structure. Consider the curves in Fig. 2 for the diluted SPEs in the region between 60 and 120 °C, where the SPEs are in a fully amorphous state. The conductivity of the SPE made from salt **2** in which two imide anions are linked by a perfluorobutane-1,4-diyl chain is diminished relative to that of an SPE made using LiTFSI by more than half an order of magnitude. However, the conductivity of SPEs made using salts **3** and **4**, in which the perfluorobutane-1,4-diyl chain in salt **2** is replaced by longer perfluorohexane-1,6-diyl or perfluorooctane-1,8-diyl chains (respectively), increases as the linker chain length increases. A similar observation was noted earlier for non-crosslinked PEO-based SPEs using the same dilithium salts[48]. Inspection of the VTF fitting parameters in Table I lends some insight; the *A*-value for salt **3** is around three times larger than that for salt **2**, and that for salt **4** is four times larger than that for salt **2**. The apparent activation energy values, Δμ, are just slowly increasing with the linker chain increase and are on average four-fold higher than those corresponding to PEO-based SPEs which signify a strong inhibition of the segmental motion of the polymer segments due to crosslinking.

With an increase in salt concentration (EO/Li = 10:1) we see, as shown in Fig. 3, a dramatic change in the dependence of ionic conductivity on the length of the linker chain. The conductivity of the SPE made from salt **2** (x = 4) is lower than that of an SPE made using LiTFSI by almost one order of magnitude, while surprisingly the conductivity of SPEs made using salts **3** (x = 6) and **4** (x = 8) decreases as the linker chain length increases, which is the opposite of what has been observed earlier for PEO-based SPEs using the same dilithium salts[47,48]. Looking at the VTF fitting parameters in Table II we observe that the *A*-value for salt **2** is around two and a half times larger than that for salts **3** and **4**, while the apparent activation energy values, Δμ, are still slowly increasing with the linker chain increase and are an average 20% lower than those corresponding to PEO-based SPEs[47] (PEG has a much lower molecular weight as compared to PEO –

a three orders of magnitude difference) and just around 30% higher than the values for the diluted SPEs.

This fact confirms the increase in the friction/entanglements of the polymeric segments with increasing anion size and concentration, lowering even more the reduced segmental motion of the crosslinked polymer and decreasing at the same time anion contribution to the overall ionic conductivity.

The behavior of SPEs made using salt **1** ($x = 2$) shows a certain distinctiveness of its ionic conductivity properties that will be discussed later. For both diluted and concentrated SPEs its conductivity is placed between those of salt **2** and **3**, which is most probably due to the formation of two non-interacting anions linked together structure as compared with more like extended delocalized dianions for salts **2**–**4**.

Electronic Structure and Ion Dissociation Energy Calculations of Dilithium Bis(perfluoroalkanesulfonyl)diimide Salts

Based on our previous work done with SPEs prepared using dilithium sulfonimide salts and high-molecular-weight PEO [47,52], we considered in greater depth, using computational approaches[59], the question of substituent effects on dianionic sulfonimide-based lithium salts (**1**–**4**). There has been prior computational work focusing on TFSI anion[35,45,60–62] and related sulfonimide species[63,64]; however, none has focused on the regular variations in properties expected with systematic structure changes of these salts (e.g., perfluoroalkylene chain length connecting the two TFSI fragments). Also, there has been no prior computational work on the related sulfonimide dianion structures. Minimum-energy conformations were calculated for lithium salts in an ion-paired form in which lithium ions were removed from the imide nitrogen but remained in the vicinity of the sulfonimide anions. The calculations also provided values for the ion dissociation enthalpy, e.g., the energy change associated with conversion from a species with lithium bound to nitrogen into a species with lithium ion-paired to the sulfonimide anion. Trends in this enthalpy change with respect to perfluoroalkylene chain length were evaluated for a series of dilithium sulfonimide salts of type Li_2X (salts **1**–**4**). A strong electron-withdrawing effect of long-chain perfluoroalkylene substituents on sulfonimide dianions was found. This effect should promote stabilization of negative charge in dissociated sulfonimide salts which should favor salt dissociation and high conductivity in low-dielectric media such as polymer (in particular polyether) hosts.

All calculations were performed using the density functional theory (DFT) under the generalized gradient approximation using the BLYP functional. Double numerical basis sets augmented with polarization functions were used for all electrons (core electrons included). All molecules were fully optimized to obtain the minimum energy structures. For some of the long-chain molecules, the conformational stability was also studied, such that the structures obtained for these molecules are very near the global minimum.

Calculations focused on the energy change associated with lithium ion dissociation from the imide nitrogen in these salts to give charge-separated ion pair species. For the dilithium salts **1**–**4** dissociation proceeds in two discrete steps, as indicated in Eqs (*3*) and (*4*).

$$CF_3SO_2N(Li)[SO_2(CF_2)_xSO_2N(Li)]SO_2CF_3 \rightarrow$$
$$\rightarrow CF_3SO_2N^{\ominus}[SO_2(CF_2)_xSO_2N(Li)]SO_2CF_3 + Li^{\oplus} \qquad (3)$$

$$CF_3SO_2N^{\ominus}[SO_2(CF_2)_xSO_2N(Li)]SO_2CF_3 \rightarrow$$
$$\rightarrow CF_3SO_2N^{\ominus}[SO_2(CF_2)_xSO_2N^{\ominus}]SO_2CF_3 + Li^{\oplus} \qquad (4)$$

In all cases the energy changes associated with lithium dissociation are linked to specific minimum-energy structures which are derived from electronic structure calculations. As will be shown below, all of the fully optimized molecular structures have lithium atoms essentially fully dissociated from the nitrogen atoms but coordinated by nearby two oxygen atoms from sulfonyl groups. In a minimum-energy structure for the Li_2X-type salt, both sulfonimide groups are dissociated into individual, discrete ion pairs with lithium coordinated by two oxygen atoms from each sulfonimide anion. Also, in all cases the energy changes associated with lithium dissociation are endothermic, meaning that it is energetically disfavored for lithium ions to dissociate. This result seems counterintuitive since salt dissociation is required in a battery electrolyte; however, it is simply a consequence of the fact that the calculations were done in the gas phase and therefore do not account for both ion solvation and ion-polymer interactions. Ion dissociation would become favorable if the solvation energy of the separated anions and cations was considered. The critical parameters in

these calculations are the changes in reaction energy within the series as the length of the perfluoroalkylene chains in the various salts is systematically changed. A shift to less endothermic reaction energies (less positive ΔE_{diss}) indicates that lithium dissociation is less disfavored (more favored), which in a solvating environment would favor a greater extent of salt dissociation.

Figure 6a illustrates the dissociation energy variation (ΔE_{diss} in kcal/mol) with chain length for the first lithium ion dissociation step in the salts **1**–**4** series. The trend for this series shows that lithium dissociation proceeds easier when the perfluoroalkylene linker chain length is shorter and becomes more endothermic as chain length increases. This at the first glance is counterintuitive since longer $(CF_2)_x$ chains are more electron-withdrawing and thus should facilitate the ionization process.

However, a shorter $(CF_2)_x$ chain has the advantage of being closer to the highly electron-withdrawing SO_2–N–SO_2 group on both sides, which facilitates the negative charge redistribution onto the entire molecule upon the first ionization. Figure 6b provides support for this idea in the form of a plot of fragment Mulliken charges on the $CF_3SO_2N^{\ominus}SO_2$–$(CF_2)_x$ units as a function of chain length. As the perfluoroalkylene chain becomes long the fragment charge on this unit approaches –1, whereas for shorter chains some of the charge spills over and becomes localized on the $SO_2N(Li)SO_2CF_3$ fragment. The extra stabilization of negative charge by the second sulfonimide is thus most effective when the linker between the two sulfonimide units is shortest. The short chain makes the overall anion species for the first ionization step more charge-balanced and thus more stable.

The second lithium dissociation brings about a return to the general behavior expected for this series, less endothermic dissociation energies as perfluoroalkylene chain length increases. This trend is illustrated in Fig. 7a via a plot showing the variation of ΔE_{diss} with chain length (x) for the second lithium ion dissociation step in the salt series **1**–**4**. Interestingly, this effect appears not to be leveling off at eight perfluoromethylene units, which suggests that further stabilization of negative charge may be possible in dianionic or polyanionic salts by using even longer perfluoroalkylene linking groups.

Finally, Fig. 7b presents a plot of fragment Mulliken charges on the interior perfluoroalkylene chain as a function of chain length for the fully dissociated, dianionic form of the salt. As might be expected, the fractional negative charge on the chain increases as the chain length increases. The average energy change to separate a pair of lithium cations from the dilithium salts **1**–**4** is shown in Fig. 8. Overall, the average energy change

decreases as the chain length increases. We expect that the use of long-chain perfluorinated substituents will be much more effective in promoting salt dissociation in dianionic and polyanionic salts than in monoanionic salts.

The insights provided by these findings help us to understand the previously reported trends in ionic conductivity of solid polymer electro-

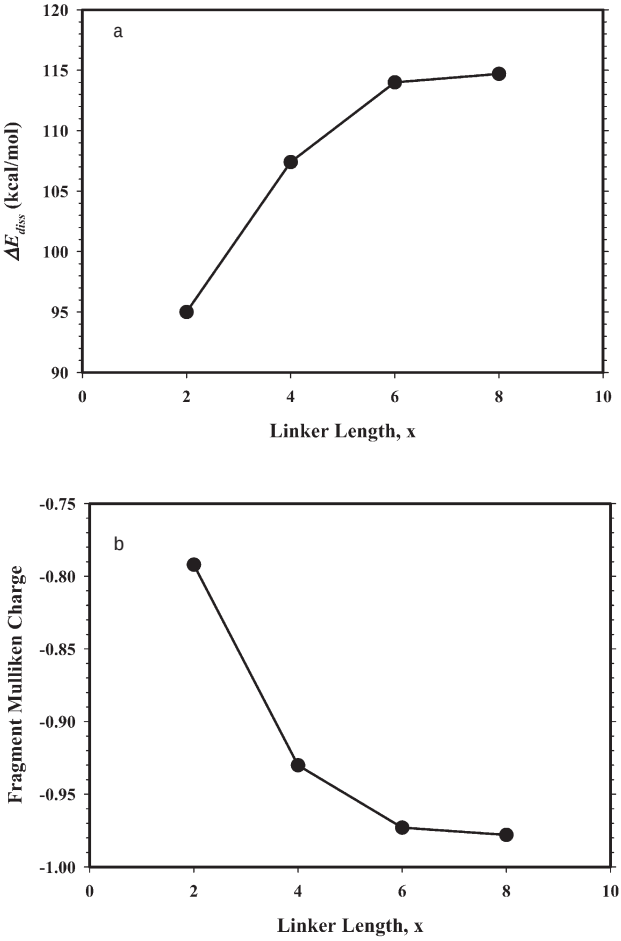

FIG. 6

a Dissociation energy values for the first lithium dissociation step (Eq. (*3*)) vs *x*, the number of perfluoromethylene groups connecting the two sulfonimide units together in salts **1**–**4**. b Fragment Mulliken charges on the $CF_3SO_2N^{\ominus}SO_2$–$(CF_2)_x$– portion of singly-dissociated salts of structure $CF_3SO_2N^{\ominus}SO_2$–$(CF_2)_x$–$SO_2N(Li)SO_2CF_3$

lytes prepared in polyether hosts using a series of dianionic salts like $CF_3SO_2N(Li)SO_2–(CF_2)_x–SO_2N(Li)SO_2CF_3$ with x = 2, 4, 6, 8 (salts **1**–**4**)[10,47,48].

Also, ionic conductivities for the salts **2**–**4** have been measured in dilute acetonitrile solutions (10^{-3}–10^{-4} mol/l) in the 25–40 °C temperature range. The main observation, similar to that of the polyanionic series[53], was that both molar conductivities and ionic conductivities decreased with increas-

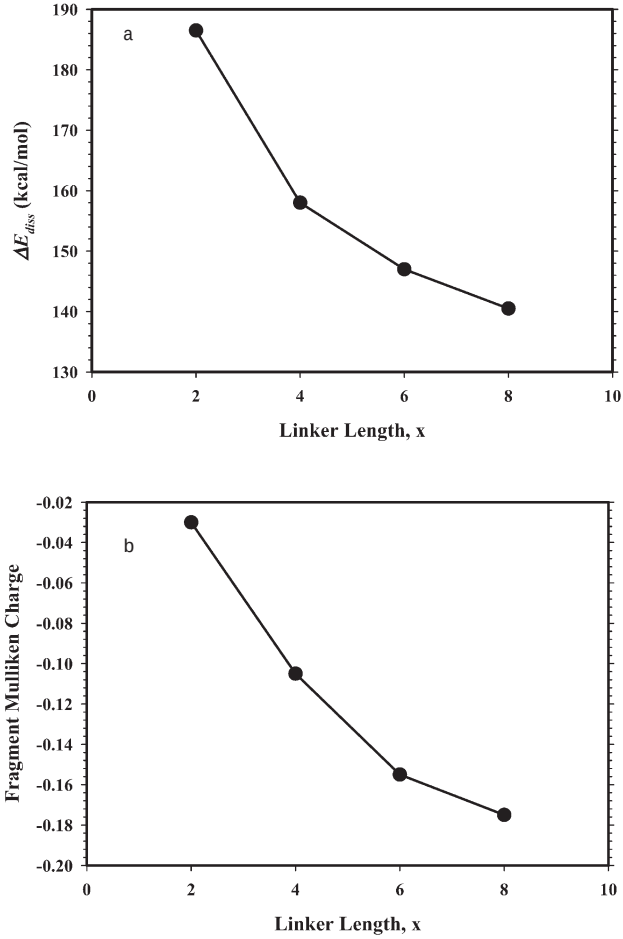

FIG. 7

a Dissociation energy values for the second lithium dissociation step (Eq. (*4*)) vs x, the number of perfluoromethylene groups connecting the two sulfonimide units together in salts **1**–**4**. b Fragment Mulliken charges on the $–(CF_2)_x–$ fragment as a function of x

ing the perfluoromethylene linker length from 4 to 6 to 8 over the entire concentration range. In the high-electric-permittivity acetonitrile (ε = 36) the salts were totally dissociated and the conductivities depended exclusively on the salt diffusion coefficient (which is proportional to the reciprocal square root of the lithium salt molecular weight)[48].

The Arrhenius plots for SPEs using these salts and as a polymeric host either low-molecular-weight cross-linked PEG (M = 2 × 10^3) or high-molecular-weight PEO (M = 4 × 10^6) in two salt concentrations (EO/Li = 30:1 and 10:1) were already presented in Figs 2 and 3 and in our previous work[10,48], respectively. Ionic conductivity data at any given temperature shows a monotonic increase with increasing perfluoromethylene linker length from 4 to 6 to 8 for PEO-based SPEs and for diluted crosslinked PEG-based SPEs (30:1) while for concentrated crosslinked PEG-based SPEs (10:1) the order is inversed, from 8 to 6 to 4. An activation analysis using the VTF formalism (Tables I and II and the information previously published in[10,48], respectively) revealed that the increased conductivity is associated mainly with an increase in the population of charge carriers (*A*-values), which probably correlates with different degrees of salt dissociation. Also, for salt **1** can be seen from Fig. 7b that the fragment Mulliken charge on the $(CF_2)_x$ linker is several times (3.5–6) lower than for salts **2**–**4** which backs up a previous assertion that the latter have a more delocalized

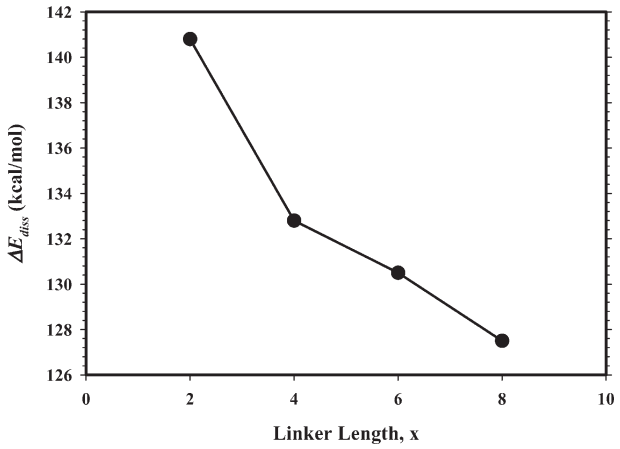

FIG. 8

Average dissociation energy values, normalized on a per-lithium basis, for the overall two-lithium dissociation steps (Eqs (*3*) and (*4*)) vs *x*, the number of perfluoromethylene groups connecting the two sulfonimide units together in dilithium salts **1**–**4**

behavior than salt **1**. Calculations from this modeling/simulation work are completely consistent with this interpretation, indeed barring any other effects that might be operative, e.g., different anion mobilities for anions of different sizes, and they suggest that the use of even longer perfluoroalkylene linkers should provide further improvements in salt dissociation and ionic conduction.

CONCLUSIONS

Solid polymer electrolytes have been prepared from a series of new dimeric dilithium bis(perfluoroalkanesulfonyl)diimide salts using crosslinked low-molecular-weight poly(ethylene glycol) as the polymer host. Ionic conductivities for the SPEs were measured over a temperature range between ambient temperature and 120 °C. The highest conductivities were generally found for SPEs with the highest salt content. Conductivities of SPEs made using the dimeric salts were consistently lower than for comparable SPEs prepared using the monomeric salt LiTFSI, which probably reflects a diminished contribution of the anions in the dimeric salts to the overall conductivity. An unexpected finding of increasing ionic conductivity with increasing the content of fluorine in the dianions is thought to be the result of two opposing trends, one reflecting an increase in anion size with an increased content of fluorine which diminishes anion transport and conductivity, and another reflecting an increase in anion basicity with increased fluorination which results in diminished ion pairing and an enhancement in the number of charge carriers, thereby increasing conductivity.

Though crosslinking decreased the ionic conductivity it improved the dimensional stability and the mechanical properties for all electrolytes. Still the LiTFSI-based SPEs exhibited the highest ionic conductivity for the entire concentration and temperature ranges. Due to the network created by crosslinking, SPEs based on dilithium salts **1**–**4** (x = 2, 4, 6, 8) showed an ionic conductivity that relied on both linker chain length (x) and salt concentration (EO/Li). Therefore, ionic conductivity values increased over the entire temperature range with the size of dianion for the diluted SPEs (30:1), while for the concentrated electrolytes (10:1) the trend was reversed due to a stronger interaction with the 3D polymer network generated by crosslinking (increasing activation energies which were not anymore compensated by an increase in the concentration of the charge carriers as the anion size increased).

Additionally, modeling/simulation work using the density functional theory, evaluated the enthalpy change with respect to perfluoroalkylene chain length for this series of dilithium sulfonimide salts **1**–**4** in gas phase. The calculations provided values for both ion dissociation enthalpies, e.g., the energy change associated with conversion from a species with lithium bound to nitrogen into a species with lithium ion-paired to the sulfonimide anion. The trends in the enthalpy change with respect to perfluoroalkylene chain length were compared with the experimental data providing an important tool for understanding the structure/properties relationship.

The authors are grateful for the financial support of this research by the DoD (Grant No. DAAG 55-98-1-Q004) and the DOE (BATT Program – Grant No. DE-AC03-76SF00098).

REFERENCES

1. Wright P. V.: *Br. Polym. J.* **1975**, *7*, 319.
2. Armand M.: *Solid State Ionics* **1983**, *9/10*, 745.
3. Ratner M. A., Shriver D. F.: *Chem. Rev.* **1988**, *88*, 109.
4. Neidi R. J. in: *Modern Battery Technology* (C. D. S. Tuck, Ed.). Ellis Horwood, New York 1991.
5. del Río C., Acosta J. L.: *Polym. Bull.* **1997**, *38*, 63.
6. Gray F. M.: *Solid Polymer Electrolytes – Fundamentals and Technological Applications*. VCH, New York 1991.
7. Gray F. M.: *Polymer Electrolytes*. The Royal Society of Chemistry, Cambridge 1997.
8. Spotnitz R. in: *Advances in Lithium-Ion Batteries* (W. A. van Schalkwijk and B. Scrosati, Eds), p. 433. Kluwer Academic/Plenum Publishers, New York 2002.
9. Mastragostino M., Soavi F., Arbizzani C. in: *Advances in Lithium-Ion Batteries* (W. A. van Schalkwijk and B. Scrosati, Eds), p. 481. Kluwer Academic/Plenum Publishers, New York 2002.
10. Geiculescu O. E., Creager S. E., DesMarteau D. D.: *Fluorinated Materials for Energy Conversion* (T. Nakajima and H. Groult, Eds). Elsevier, Amsterdam 2005.
11. Wong S., Vaia R. A., Giannelis E. P., Zax D. B.: *Solid State Ionics* **1996**, *86*, 547.
12. Minier M., Berthier C., Gorecki W.: *J. Phys.* **1984**, *45*, 739.
13. Berthier C., Gorecki W., Minier M., Armand M. B., Chabagno J. M., Rigaud P.: *Solid State Ionics* **1983**, *11*, 91.
14. Gorecki W., Donoso P., Berthier C., Mali M., Roos J., Brinkmann D., Armand M. B.: *Solid State Ionics* **1988**, *28–30*, 1018.
15. Wintersgill M. C., Fontanella J. J., Pak Y. S., Greenbaum S. G., Almudaris A., Chadwick A. V.: *Polymer* **1989**, *30*, 1123.
16. Nagaoka K., Naruse H., Shinohara I., Watanabe M.: *J. Polym. Sci. Polym. Lett.* **1984**, *22*, 659.
17. Przuski J., Wieczorek W.: *Solid State Ionics* **1992**, *53*, 1071.
18. Blonsky P. M., Shriver D. F., Austin P. E., Allcock H. R.: *J. Am. Chem. Soc.* **1984**, *106*, 6854.

19. Gray F. M., MacCallum J. R., Vincent C. A., Giles J. R. M.: *Macromolecules* **1988**, *21*, 392.
20. Le Nest J.-F., Gandini A., Cheradame H.: *Br. Polym. J.* **1988**, *20*, 253.
21. Le Nest J.-F., Callens S., Gandini A., Armand M.: *Electrochim. Acta* **1992**, *37*, 1585.
22. Gadjourova Z., Andreev Y. G., Tunstall D. P., Bruce P. G.: *Nature* **2001**, *412*, 520.
23. Staunton E., Andreev Y. G., Bruce P. G.: *Faraday Discuss.* **2007**, *134*, 143.
24. Stoeva Z., Martin-Litas I., Staunton E., Andreev Y. G., Bruce P. G.: *J. Am. Chem. Soc.* **2003**, *125*, 4619.
25. Killis A., Le Nest J. F., Cheradame H.: *Makromol. Chem. Rapid Commun.* **1980**, *1*, 595.
26. Borghini M. C., Mastragostino M., Zanelli A.: *Electrochim. Acta* **1996**, *41*, 2369.
27. Carvalho L. M., Guegan P., Cheradame H., Gomes A. S.: *Eur. Polym. J.* **1997**, *33*, 1741.
28. Laik B., Legrand L., Chausse A., Messina R.: *Electrochim. Acta* **1998**, *44*, 773.
29. Valee A., Besner S., Prud'homme J.: *Electrochim. Acta* **1992**, *37*, 1579.
30. Sylla S., Sanchez J.-Y., Armand M.: *Electrochim. Acta* **1992**, *37*, 1699.
31. Salomon M.: *J. Solution Chem.* **1993**, *22*, 715.
32. Lascaud S., Perrier M., Valee A., Besner S., Prud'homme J., Armand M.: *Macromolecules* **1994**, *27*, 7469.
33. Gorecki W., Jeannin M., Belorizky E., Roux C., Armand M.: *J. Phys.: Condens. Matter* **1995**, *7*, 6823.
34. Andreev Y. G., Lightfoot P., Bruce P. G.: *Chem. Commun.* **1996**, *18*, 2169.
35. Rey I., Johansson P., Lindgren J., Lassegues J. C., Grondin J., Servant L.: *J. Phys. Chem. A* **1998**, *102*, 3249.
36. Brouillette D., Perron G., Desnoyers J. E.: *J. Solution Chem.* **1998**, *27*, 151.
37. Edman L., Doeff M. M., Ferry A., Kerr J., De Jonghe L. C.: *J. Phys. Chem. B* **2000**, *104*, 3476.
38. Zhang S., Chang Z., Xu K., Angell C. A.: *Electrochim. Acta* **2000**, *45*, 1229.
39. Armand M., Gorecki W., Andreani R.: Presented at *Second International Symposium on Polymer Electrolytes, New York 1990*.
40. Nagasubramanian G., Shen D. H., Surampudi S., Wang Q., Syrya Prakash G. K.: *Electrochim. Acta* **1995**, *40*, 2277.
41. Armand M. B. in: *Polymer Electrolyte Reviews* (J. R. MacCallum and C. A. Vincent, Eds), Vol. 1. Elsevier Applied Science, London and New York 1987.
42. Abraham K. M. in: *Applications of Electroactive Polymers* (B. Scrosati, Ed.). Chapman & Hall, London 1993.
43. Perrier M., Besner S., Paquette C., Vallee A., Lascaud S., Prud'homme J.: *Electrochim. Acta* **1995**, *40*, 2123.
44. Dai H., Zawodzinski T. A.: *J. Electroanal. Chem.* **1998**, *459*, 111.
45. Zhang J., DesMarteau D. D.: *J. Fluorine Chem.* **2001**, *111*, 253.
46. Zhang J., DesMarteau D. D., Zuberi S., Ma J.-J., Xue L., Gillette S. M., Blau H., Gerhardt R.: *J. Fluorine Chem.* **2002**, *116*, 45.
47. Geiculescu O. E., Xie Y., Rajagopal R. V., Creager S. E., DesMarteau D. D.: *J. Fluorine Chem.* **2004**, *125*, 1179.
48. Geiculescu O. E.: *Ph.D. Thesis*. Clemson University, Clemson 2004.
49. DesMarteau D. D.: *J. Fluorine Chem.* **1995**, *72*, 203.
50. Macdonald J. R., Johnson W. B. in: *Impedance Spectroscopy* (J. R. Macdonald, Ed.). John Wiley & Sons, New York 1987.
51. Watanabe M., Ogata N. in: *Polymer Electrolytes Reviews* (J. R. MacCallum, Ed.), Vol. 1. Elsevier Applied Science, London and New York 1987.

52. Geiculescu O. E., Yang J., Blau H., Bailey-Walsh R., Creager S. E., Pennington W. T., DesMarteau D. D.: *Solid State Ionics* **2002**, *148*, 173.
53. Geiculescu O. E., Yang J., Zhou S., Shafer G., Xie Y., Albright J., Creager S. E., Pennington W. T., DesMarteau D. D.: *J. Electrochem. Soc.* **2004**, *151*, A1363.
54. West K., Christiansen B. Z., Jacobsen T., Hiort-Lorenzen E., Skaarup S.: *Br. Polym. J.* **1988**, *20*, 243.
55. Hubbard H. V. S. A., Southall J. P., Cruickshank J. M., Davies G. R., Ward I. M.: *Electrochim. Acta* **1998**, *43*, 1485.
56. Papke B. L., Ratner M. A., Shriver D. F.: *J. Electrochem. Soc.* **1982**, *129*, 1694.
57. Shriver D. F., Dupon R., Stainer M.: *J. Power Sources* **1983**, *9*, 383.
58. Linford R. G. in: *Applications of Electroactive Polymers* (B. Scrosati, Ed.). Chapman & Hall, London 1993.
59. Creager S. E.: Unpublished results.
60. Johansson P., Gejji S. P., Tegenfeldt J., Lindgren J.: *Electrochim. Acta* **1998**, *43*, 1375.
61. Gejji S. P., Suresh C. H., Babu K., Gadre S. R.: *J. Phys. Chem. A* **1999**, *103*, 7474.
62. Johansson P., Jacobsson P.: *J. Phys. Chem. A* **2001**, *105*, 8504.
63. Johansson P., Tegenfeldt J., Lindgren J.: *J. Phys. Chem. A* **2000**, *104*, 954.
64. Johansson P.: *J. Phys. Chem. A* **2001**, *105*, 9258.